Enhancement of four-wave mixing process in a four-level double semiconductor quantum well*

She Yan-Chao(佘彦超)[a)b)], Zheng Xue-Jun(郑学军)[a)b)†], and Wang Deng-Long(王登龙)[a)b)‡]

[a)] *Faculty of Materials, Optoelectronics and Physics, Xiangtan University, Xiangtan* 411105, *China*

[b)] *Key Laboratory of Low Dimensional Materials and Application Technology of the Ministry of Education, Xiangtan University, Xiangtan* 411105, *China*

(Received 11 March 2014; revised manuscript received 26 April 2014; published online 10 October 2014)

The time-dependent four-wave mixing (FWM) is analyzed in a four-level double semiconductor quantum well. The results show that both the amplitude and the conversion efficiency of the FWM field are enhanced with increasing the strength of two-photon Rabi frequency. Interestingly, when the one-photon detuning becomes stronger the control field corresponding to the maximum efficiency increases. Such a controlled enhanced FWM may be used to generate coherent short-wave length radiation, and it can have potential applications in quantum control and communications.

Keywords: electromagnetically induced transparency, semiconductor quantum wells, four-wave mixing

PACS: 42.50.Gy, 78.67.De, 42.65.–k **DOI:** 10.1088/1674-1056/23/12/124202

1. Introduction

During the last decade, the electromagnetically induced transparency (EIT) in a resonant optical medium has been a point of attraction because of its potential applications in quantum information processing and transmission.[1–3] The optical field propagation in the optical medium under EIT configuration displays several striking features, including a large suppression of optical absorption, a significant reduction of group velocity, and a giant enhancement of Kerr nonlinearity, etc.[4–12] Based on these interesting features, four-wave mixing (FWM), as one of the striking nonlinear quantum optical phenomena, has been explored recently in the EIT media because of its potential applications in frequency conversion, quantum entanglement, and stopped light.[13–18] The first experimental demonstration of EIT-based FWM was reported by Zhang *et al*., and then a significant enhancement of the FWM process by using EIT was observed in rubidium atomic vapor.[13] Later on, Deng *et al*. proposed an FWM scheme based on EIT and the associated slow light propagation, and their calculations showed that many orders of magnitude increase in the FWM efficiency may be obtained.[14] Quite recently, Li and Huang proposed a scheme to obtain a highly efficient FWM in a coherent five-level tripod system by using a double-dark resonance and multiphoton destructive interference-induced transparency.[15] However, most of these previous investigations on the field of multi-wave mixing focused on the passive optical medium and cold atomic medium.[13–22] For low efficiency and low operating temperature in cold atomic medium, the multi-wave mixing cannot be conveniently used in devices with good scalability. It is interesting to extend the study on multi-wave mixing to solid-state systems, including semiconductor quantum wells (QW) and quantum dots. Much of the recent literature has exploited semiconductor quantum well (SQW) structure.[23,24] In this type of system, the discrete energy levels and optical properties are closely analogous to those in atomic systems. Furthermore, it is intriguing to note that the SQW structure also has inherent advantages such as large electric dipole moment, high nonlinear optical coefficient, widely adjustable parameter, and flexibility.

Motivated by those important properties, we try to study systematically the high-efficiency FWM process in this specific system, and whether it is more promising for practical applications.[25–30] In this paper, a detailed study of the four-wave mixing (FWM) process is presented and the generated FWM field is investigated from the amplitude and conversion efficiency in a four-level coupled GaAs/AlGaAs quantum well based on the EIT effect. We expect to present a controlled high-efficiency FWM process in the SQW structure, and it may be useful to generate coherent short-wave length radiation in solid material. The rest of this paper is arranged as follows. In Section 2, we describe the four-level coupled GaAs/AlGaAs quantum well model and derive the nonlinear equation governing the motion of the envelope of the probe field and FWM field. In Section 3, we present analytical solution and propaga-

*Project supported by the Program for Changjiang Scholars and Innovative Research Team in University, China (Grant No. IRT1080), the National Natural Science Foundation of China (Grant Nos. 51272158, 11374252, and 51372214), the Changjiang Scholar Incentive Program, China (Grant No. [2009]17), the Shanghai Nano Special Foundation, China (Grant No. 11nm0502600), the Scientific Research Fund of Hunan Provincial Education Department, China (Grant No. 12A140), the Science and Technology Foundation of Guizhou Province, China (Grant No. J20122314), and the Hunan Provincial Innovation Foundation for Postgraduate, China (Grant No. CX2012B248).

†Corresponding author. E-mail: zhengxuejun@xtu.edu.cn

‡Corresponding author. E-mail: dlwang@xtu.edu.cn

© 2014 Chinese Physical Society and IOP Publishing Ltd

tion characteristics of FWM. The controllability of the conversion efficiency of the generated FWM is also discussed by manipulating the driven field and one-photon detuning. Finally, in Section 4, brief discussion is made and some conclusions are drawn from the present study.

2. Model

We here consider the properties of FWM in an n-doped asymmetric GaAs/AlGaAs double SQW structure,[24] and it interacts with a weak pulsed pump field (ω_p), a strong continuous-wave (CW) control field (ω_c), and a driven field (ω_d), as shown in Fig. 1. This structure consists of an $Al_{0.04}Ga_{0.96}As$ layer (shallow well) with a thickness of 11.0 nm and a 9.5-nm GaAs layer (deep well), and they are separated by a 3.8-nm $Al_{0.4}Ga_{0.6}As$ potential barrier. Both the left side of the shallow well and the right side of the deep well are $Al_{0.4}Ga_{0.6}As$ potential barriers.[24] The probe and the control fields couple with the transitions $|1\rangle \leftrightarrow |4\rangle$ and $|2\rangle \leftrightarrow |4\rangle$ respectively, and the driven field provides a two-photon coupling the transition $|3\rangle \leftrightarrow |4\rangle$. In this structure, $|1\rangle$ and $|2\rangle$ are the ground subbands of the left shallow and the right deep wells respectively. Two subbands $|3\rangle$ and $|4\rangle$ are created by mixing the first excited subbands of the shallow and deep wells through the resonant tunneling. The probe field and the resonant two-photon field induce an FWM process $|1\rangle \rightarrow |4\rangle \rightarrow |3\rangle \rightarrow |1\rangle$, then generate a coherent radiation field at frequency ω_m with $\omega_m = \omega_p - 2\omega_d$. Here, ω_p and ω_d are the central frequencies of weak pulsed pump field and the two-photon driven field, respectively. Subbands $|1\rangle$, $|2\rangle$, and $|4\rangle$ form the usual EIT scheme together with the weak probe and CW control fields. The four conduction subbands of the SQW under consideration are represented in real space as an ensemble of four levels localized at the atomic sites of the two-dimensional SQW. Considering a simple case in which the electrons occupy their states as independent particles, the dynamic behaviors of electrons can be described by equations of motion for probability amplitudes. By using the rotating wave approximation,[5,15,27] the dynamic behaviors of the slowly varying probability amplitudes $A_{j=2,3,4}$ are governed by

$$\mathrm{i}\frac{\partial A_2}{\partial t} + d_2 A_2 + \Omega_c A_4 = 0, \tag{1a}$$

$$\mathrm{i}\frac{\partial A_3}{\partial t} + d_3 A_3 + \Omega_m A_1 + \Omega_d^{(2)} A_4 = 0, \tag{1b}$$

$$\mathrm{i}\frac{\partial A_4}{\partial t} + d_4 A_4 + \Omega_p A_1 + \Omega_d^{(2)} A_3 + \Omega_c A_2 = 0, \tag{1c}$$

where $d_2 = \Delta_p - \Delta_c + \mathrm{i}\gamma_2$, $d_3 = \Delta_m + \mathrm{i}\gamma_3$, $d_4 = \Delta_p + \mathrm{i}\gamma_4$. $\Delta_{p(c,m)} = \omega_{p(c,m)} - \omega_{41(42,31)}$ are the single-photon detunings; $\gamma_{j=2,3,4}$ and $\Omega_d^{(2)} = p_{43}\varepsilon_d/\hbar$ are the total electron decay rate of subbands $|j\rangle$ and the direct two-photon Rabi frequency from subband $|3\rangle$ to $|4\rangle$; $\Omega_c = p_{42}\varepsilon_c/2\hbar$, $\Omega_p = p_{41}\varepsilon_p/2\hbar$, and $\Omega_m = p_{31}\varepsilon_m/2\hbar$ are the half Rabi frequencies of the control, pump and FWM field, respectively. Here, $p_{43} = \boldsymbol{e}_d \cdot \boldsymbol{p}_{43}$, $p_{42} = \boldsymbol{e}_c \cdot \boldsymbol{p}_{42}$, $p_{41} = \boldsymbol{e}_p \cdot \boldsymbol{p}_{41}$, and $p_{31} = \boldsymbol{e}_m \cdot \boldsymbol{p}_{31}$ are the dipole moments of transitions $|3\rangle \leftrightarrow |4\rangle$, $|2\rangle \leftrightarrow |4\rangle$, $|1\rangle \leftrightarrow |4\rangle$, and $|1\rangle \leftrightarrow |3\rangle$ respectively, where $\boldsymbol{e}_{c,p,m,d}$ is the unit vector denoting the polarization of the laser field, with the envelope $\varepsilon_{c,p,m,d}$.

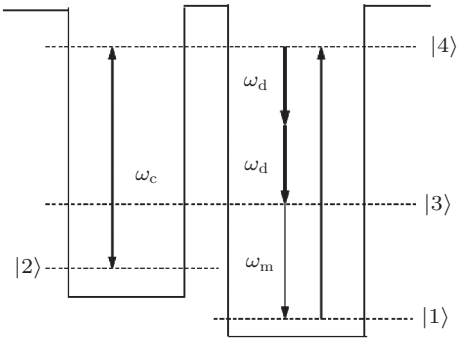


Fig. 1. Schematic energy-level diagram in a double SQW structure interacting with a strong control field coupling with the transition $|2\rangle \leftrightarrow |4\rangle$ (with carrier frequency ω_c) and a weak probe optical field coupling with the transition $|1\rangle \leftrightarrow |4\rangle$ (with carrier frequency ω_p). The subband $|3\rangle$ couples with $|4\rangle$ by a two-photon process (with carrier frequency $2\omega_d$).

In order to describe the propagation characteristics of the generated FWM, the motion equations must be simultaneously solved with Maxwell's equation in a self-consistent manner.[31] Under a slowly varying envelope approximation, we obtain

$$\mathrm{i}\left(\frac{\partial}{\partial z} + \frac{1}{c}\frac{\partial}{\partial t}\right)\Omega_p + \kappa_{14} A_1^* A_4 = 0, \tag{2a}$$

$$\mathrm{i}\left(\frac{\partial}{\partial z} + \frac{1}{c}\frac{\partial}{\partial t}\right)\Omega_m + \kappa_{13} A_1^* A_3 = 0. \tag{2b}$$

Here $\kappa_{13(14)} = N_a \omega_{m(p)} \left|p_{13(14)}\right|^2 / (2\varepsilon_0 \hbar c)$ are the propagation coefficients, with c and N_a being the speed of light in vacuum and the electron density in the valence band of the quantum well, respectively. For simplicity, we assume that the CW control field is strong enough and stable so that Ω_c can be regarded as a constant.

3. Propagation characteristics of FWM

Considering the phase-matched condition, the solution of the FWM problem is studied based on Eqs. (1) and (2). We assume that the probe field is weak and the ground state of the system is not depleted, i.e., $A_1 \approx 1$. By using the Fourier transform

$$A_j = \frac{1}{\sqrt{2\pi}} \int_{-\infty}^{+\infty} \alpha_j \exp(-\mathrm{i}\omega t)\,\mathrm{d}\omega \quad (j = 2-4)$$

and $\Omega_{p(m)} = \frac{1}{\sqrt{2\pi}} \int_{-\infty}^{+\infty} \Lambda_{p(m)} \exp(-\mathrm{i}\omega t)\,\mathrm{d}\omega$,[13] from Eqs. (1) and (2), we have

$$f_2 \alpha_2 + \Omega_c^* \alpha_4 = 0, \tag{3a}$$

$$f_3 \alpha_3 + \Lambda_m + \Omega_d^{(2)} \alpha_4 = 0, \tag{3b}$$

$$f_4\alpha_4 + \Lambda_{\rm p} + \Omega_{\rm d}^{(2)}\alpha_3 + \Omega_{\rm c}\alpha_2 = 0, \tag{3c}$$

$$\frac{\partial \Lambda_{\rm p}}{\partial z} - {\rm i}\frac{\omega}{c}\Lambda_{\rm p} = {\rm i}\kappa_{13}\alpha_3, \tag{3d}$$

$$\frac{\partial \Lambda_{\rm m}}{\partial z} - {\rm i}\frac{\omega}{c}\Lambda_{\rm m} = {\rm i}\kappa_{14}\alpha_4, \tag{3e}$$

where α_j and $\Lambda_{\rm p(m)}$ are the Fourier transforms of A_j and $\Omega_{\rm p(m)}$, respectively. $f_j = d_j + \omega$ ($j = 2$–4), and ω is the Fourier variable. Making use of the initial condition for the FWM-generated field (i.e. $\Lambda_{\rm m}(z=0) = 0$ and $\Lambda_{\rm p0} = \Lambda_{\rm p}(z = 0) \neq 0$) and combining Eq. (3), one obtains the solutions for the probe laser field and the FWM field as follows:

$$\Lambda_{\rm p} = \frac{\Lambda_{\rm p}(0,\omega)}{U_+ - U_-}[U_+\exp({\rm i}K_+ z) - U_-\exp({\rm i}K_- z)], \tag{4a}$$

$$\Lambda_{\rm m}(z,\omega) = \frac{U_+U_-}{U_+ - U_-}\Lambda_{\rm p}(0,\omega)[\exp({\rm i}K_+ z) - \exp({\rm i}K_- z)], \tag{4b}$$

with

$$U_\pm = \frac{\kappa_{13}D_{\rm c} + \kappa_{14}f_2f_3 \pm \sqrt{G}}{2\kappa_{14}f_2\Omega_{\rm d}^{(2)}}$$

and $G = (\kappa_{13}D_{\rm c} - \kappa_{14}f_2f_3)^2 + 4D\kappa_{13}\kappa_{14}f_2$. By seeking their approximated inverse Fourier transform, one obtains

$$\Omega_{\rm p}(z,t) = \frac{W_+\Omega_{\rm p}(t - z/v_{\rm g+})\,{\rm e}^{{\rm i}zK_+(0)} - W_-\Omega_{\rm p}(t - z/v_{\rm g-})\,{\rm e}^{{\rm i}zK_-(0)}}{W_+ - W_-}, \tag{5a}$$

$$\Omega_{\rm m}(z,t) = \frac{W_+W_-[\Omega_{\rm p}(t - z/v_{\rm g-})\,{\rm e}^{{\rm i}zK_+(0)} - \Omega_{\rm p}(t - z/v_{\rm g+})\,{\rm e}^{{\rm i}zK_-(0)}]}{W_+ - W_-}, \tag{5b}$$

where

$$W_\pm = \frac{\kappa_{13}D_{\rm c} + \kappa_{14}f_2f_3 \pm \sqrt{G}}{2\kappa_{14}f_2\Omega_{\rm d}^{(2)}},$$

and $v_{\rm g\pm} = 1/{\rm Re}(\partial K_\pm/\partial\omega|_{\omega=0})$ being the group velocities of the $K_\pm$.

Subsequently, the dispersion relation of the system is given by

$$K_\pm = \frac{\omega}{c} + \frac{-(\kappa_{13}D_{\rm c} - \kappa_{14}f_2f_3) \pm \sqrt{G}}{2D}, \tag{6}$$

where $D = f_2|\Omega_{\rm d}^{(2)}|^2 + f_3|\Omega_{\rm c}|^2 - f_2f_3f_4$ and $D_{\rm c} = |\Omega_{\rm c}|^2 - f_2f_4$. Thus the system allows two branches of dispersion curves K_+ and K_-. To our knowledge, the imaginary part ${\rm Im}\,K_\pm(\omega)$ of Eq. (6) characterizes the linear absorption. According to the realistic parameters in a typical double SQW, we may choose $k_{13} = k_{14} = 6.2\times10^3$ cm$^{-1}\cdot$meV, $\Delta_{\rm c} = \Delta_{\rm p} = \Delta_{\rm m} = 0.0$ meV, $\gamma_2 = \gamma_3 = 1.0$ meV, $\gamma_4 = 2.0$ meV, and $|\Omega_{\rm c}| = |\Omega_{\rm d}^{(2)}| = 5.0$ meV. So, we plot the ${\rm Im}\,K_+(\omega)$ (solid line) and ${\rm Im}\,K_-(\omega)$ (dotted line) each as a function of frequency ω as shown in Fig. 2. Notice that the absorption curves for the K_+ and K_- modes and around $\omega = 0$, are very different, i.e., the absorption of the K_- mode is much more than that of the K_+ mode for an optical thick medium. It means that the K_- mode decays very quickly and the absorption of K_+ mode is largely suppressed. The suppression of the K_+ mode of the FWM field absorption is due to the quantum destructive interference effect, which is induced by the strong control field, and this effect makes the population in the level $|4\rangle$ vanish. Hence the K_+ mode of the FWM field becomes transparent in our resonant system. The physics behind it is basically the same as EIT illustrated in Ref. [14]. Therefore, we just discuss the properties of the FWM under the consideration that K_- mode can be ignored after a very short propagation distance.

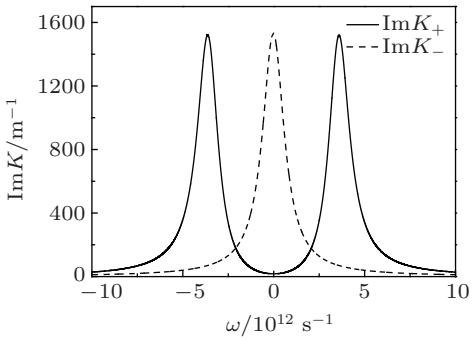


Fig. 2. The imaginary part of the dispersion relations ${\rm Im}(K_+)$ (solid curve) and ${\rm Im}(K_-)$ (dashed curve) each as a function of the frequency ω of the SQW system. The parameters of the system can be found in the text.

In order to explore the propagation characteristics of the generated FWM field, we show the normalized amplitudes of the FWM field (which is defined as $\left|\Omega_{\rm m}/\Omega_{\rm p}(z=0)\right|$)[29] as a function of the propagation distance z with different values of two-photon Rabi frequency $\Omega_{\rm d}^{(2)}$ in Fig. 3. The parameters are chosen to be $\Delta_{\rm c} = \Delta_{\rm p} = \Delta_{\rm m} = 0.0$ meV, $\gamma_2 = \gamma_3 = 1.0$ meV, $\gamma_4 = 2.0$ meV, and $|\Omega_{\rm a}| = 5.0$ meV. Our result shows that the amplitude of the generated FWM field increases monotonically with the increase of the propagation distance z, and the amplitude reaches a saturation value and is nearly independent of the propagation distance. Simultaneously, the saturation value increases with increasing the two-photon Rabi frequency $\Omega_{\rm d}^{(2)}$. This result may be understood as a competition between the creation and destruction of quantum coherences via the coupling and back-coupling excitation channels in the conduction electron system, and the amplitude of the FWM field approaches to a constant due to the balance of competition. When the generated FWM field has been sufficiently intense after a characteristic propagation distance, an efficient back-coupling excitation channel to the FWM-generated sub-

band $|3\rangle$ becomes important, which is π out of phase with respect to the coupling excitation channel. This back-coupling channel simultaneously gives rise to a destructive interference pathway, thereby suppressing the amplitude of the generated FWM subband $|3\rangle$. On the other hand, the two-photon driven field can delay or suppress the back-coupling channel, and it makes the amplitude of the FWM field reach a saturation value after a longer propagation distance. With these parameters, in addition, we can show that the group velocities of the probe and FWM fields are matched and ultraslow ($v_{\rm g}^{\rm p} = v_{\rm g}^{\rm m} \sim 10^{-3}c$). It can enhance the field-medium interaction time and also results in an increase of the FWM conversion efficiency of the system. As discussed in Refs. [14] and [24], a phase-matched FWM field can be produced if the reduced group velocity of the probe field subjected to EIT is about equal to the group velocity of the generated FWM field.

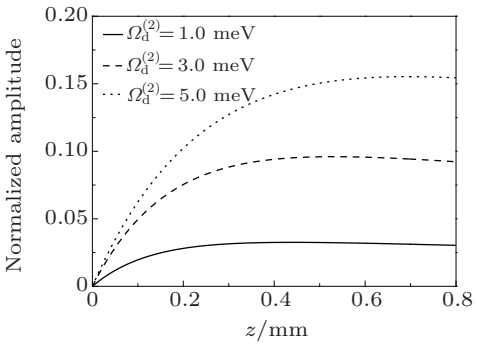


Fig. 3. Generated FWM amplitudes versus the depth z of penetration into the double SQW system for three different values of driven field $\Omega_{\rm d}^{(2)}$. The parameters of the system can be found in the text.

As discussed in Ref. [16], the FWM conversion efficiency is defined as the ratio of the energy of the output generated-FWM field to the energy of the input probe field, i.e., $\eta = |E_{\rm m}^{(\rm out)}/E_{\rm p}^{(\rm in)}|^2$. Here, $E_{\rm m}^{(\rm out)}$ is the electric field $E_{\rm m}$ ($|E_{\rm m}|^2 = 4\hbar|\Omega_{\rm m}|^2/|p_{13}|^2$) of the FWM field at the exit $z = L$ and $E_{\rm p}^{(\rm in)}$ is the electric field $E_{\rm p}$ ($|E_{\rm p}|^2 = 4\hbar|\Omega_{\rm p}|^2/|p_{14}|^2$) of the probe field at the entrance $z = 0$. Notice that the two branches of each dispersion curve are very different and the absorption of the K_+ mode is much less than that of the K_- mode for the SQW system around $\omega = 0$. Thus, after propagating a longer optical depth, the amplitude of the K_- mode decays away rapidly, hence the K_- mode can be ignored. Then equation (5) is simplified into

$$\Omega_{\rm p}(z,t) = \frac{W_+}{W_+ - W_-}\Omega_{\rm p}(t - z/v_{\rm g+})\exp({\rm i}zK_+), \quad (7a)$$

$$\Omega_{\rm m}(z,t) = \frac{W_+W_-}{W_+ - W_-}\Omega_{\rm p}(t - z/v_{\rm g+})\exp({\rm i}zK_+). \quad (7b)$$

Therefore, the FWM conversion efficiency is given by

$$\eta = \frac{|p_{13}|^2}{|p_{14}|^2}\left|\frac{2f_2\kappa_{13}\Omega_{\rm d}^{(2)}}{\kappa_{13}D_{\rm c} + \kappa_{14}f_2f_3 + \sqrt{G}}\right|^2 {\rm e}^{-2\alpha L}. \quad (8)$$

The effects of both the cross-coupling and the control fields on conversion efficiency η are considered, and the curves of efficiency η versus amplitude $|\Omega_{\rm c}|$ of the CW control field c with the different amplitude values of the driven field d are plotted in Fig. 4. For $\Omega_{\rm d}^{(2)} = 4.0$ meV, one can see that with increasing $\Omega_{\rm c}$, the conversion efficiency η first tardily increases and reaches a maximum η at $\Omega_{\rm c} \approx 5.0$ meV. It is also found that for the stronger control field (i.e., $\Omega_{\rm c} > 5.0$ meV), the conversion efficiency of the FWM field can be suppressed. A similar variation tendency of the conversion efficiency is observed with stronger driven field (e.g., $\Omega_{\rm d}^{(2)} = 5.0$ meV and $\Omega_{\rm d}^{(2)} = 6.0$ meV). Moreover, the maximum of η becomes larger when the driven field strength $\Omega_{\rm d}^{(2)}$ is stronger, while the position of the maximum nearly corresponds to that in the same control field case. Therefore, we can conclude that the conversion efficiency of the generated FWM field can be enhanced by the driven field.

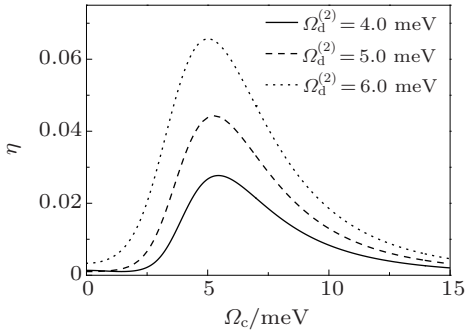


Fig. 4. Curves of conversion efficiency η of the generated FWM versus the amplitude $|\Omega_{\rm c}|$ of the CW control field c for three different values of driven field $\Omega_{\rm d}^{(2)}$. The parameters of the system can be found in the text.

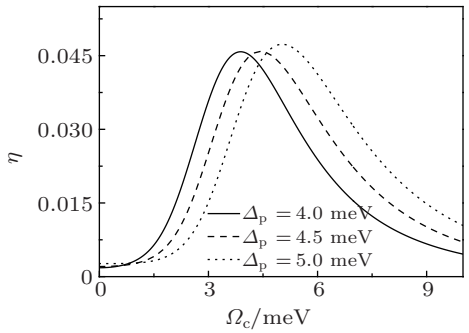


Fig. 5. Curves of conversion efficiency η of the generated FWM versus the amplitude $|\Omega_{\rm c}|$ of the CW control field c for three different values of one-photon detuning $\Delta_{\rm p}$. The parameters of the system can be found in the text.

We further show in Fig. 5 the curves of conversion efficiency η versus control field $\Omega_{\rm c}$ with the different values of one-photon detuning $\Delta_{\rm p}$. From Fig. 5 it follows that the conversion efficiency increases to a maximum and then decreases, with increasing the control field $\Omega_{\rm c}$, which is similar to the phenomenon in Fig. 4. The peak of η shifts toward the right side with the increase of $\Delta_{\rm p}$, namely, the maximum of

η does not vary with increasing the one-photon detuning Δ_p. It illustrates that detuning Δ_p may determine Ω_c where the η reaches the maximum. Such a controlled high efficiency FWM in the SQW solid state system may have potential applications in quantum control and communications.

4. Discussion and conclusion

Before drawing conclusions, we should notice that in the literature several multiple-level structures in atomic gaseous media, such as double Λ-type or tripod-type, have been proposed to investigate the high-efficiency four-wave-mixing (FWM) process. However, there are two crucial differences between our work and the previous literature, with important implications which will be mentioned here briefly. First, the medium studied in our work is a solid, which is much more practical than the gaseous medium case due to its flexible design and the controllable interference strength. Second, the transition energies, dipoles, and symmetries can be controlled at will.[33]

Now, we come to draw some conclusion from the present study. In this paper, we demonstrate the high-efficiency FWM process in a four-level SQW system by using the coupled Schrödinger–Maxwell approach. Because the EIT induced by the control field, the linear absorption of the probe, and the FWM fields can be suppressed, and their group velocities can be slowed down and matched with each other, the amplitude of the generated FWM field first increases monotonically with the increase of propagation distance z, and then reaches a saturation value. Simultaneously, the saturation value increases with increasing the two-photon Rabi frequency $\Omega_d^{(2)}$. Interestingly, with the increase of control field, the conversion efficiency exhibits parabolic change which presents a maximum value. This means that the control field can improve the conversion efficiency significantly for suitable parameter regimes. Furthermore, the maximum efficiency also increases as two-photon Rabi frequency $\Omega_d^{(2)}$ becomes stronger. Aside from this, the maximum efficiency shifts toward the larger amplitude side of the control field when the one-photon detuning Δ_p becomes stronger. The results presented in this work may be used in some areas of optical information engineering and to generate the coherent short-wavelength radiation efficiently in the SQW solid state system.

References

[1] Harris S E, Field J E and Imamoglu A 1990 *Phys. Rev. Lett.* **64** 1107
[2] Harris S E 1997 *Phys. Today* **50** 36
[3] Fleischhauer M, Imamoglu A and Marangos J P 2005 *Rev. Mod. Phys.* **77** 633
[4] Paspalakis E and Knight P L 2002 *Phys. Rev. A* **66** 015802
[5] Wu Y and Deng L 2004 *Phys. Rev. Lett.* **93** 143904
[6] Hang C and Huang G 2008 *Phys. Rev. A* **77** 033830
[7] Yang W X, Chen A X, Si L G, Jiang K, Yang X and Lee R K 2010 *Phys. Rev. A* **81** 023814
[8] She Y C, Wang D L, Zhang W X, He Z M and Ding J W 2010 *J. Opt. Soc. Am. B* **27** 208
[9] She Y C, Wang D L, Zhang W X, Zhang Z Q and Ding J W 2011 *Eur. Phys. J. D* **61** 181
[10] Hu Z F, Du C G, Li D J and Li S Q 2002 *Chin. Phys. Lett.* **19** 1805
[11] Sun J F and Li Y F 2003 *Acta Phys. Sin.* **52** 547 (in Chinese)
[12] Tu F Y, Zhang G Q, Chen C, Gao F, Bo F, Liu J B and Xu J J 2007 *Physics* **36** 399 (in Chinese)
[13] Zhang G Z, Hakuta K and Stoicheff B P 1993 *Phys. Rev. Lett.* **71** 3099
[14] Deng L, Kozuma M, Hagley E W and Payne M G 2002 *Phys. Rev. Lett.* **88** 143902
[15] Li H J and Huang G X 2007 *Phys. Rev. A* **76** 043809
[16] Wu Y, Payne M G, Hagley E W and Deng L 2004 *Opt. Lett.* **29** 2294
[17] Niu Y P, Li R X and Gong S Q 2005 *Phys. Rev. A* **71** 043819
[18] Zhang Y, Brown A W and Xiao M 2007 *Phys. Rev. Lett.* **99** 123603
[19] Zhang S A, Sun Z R, Wang Y F, Zeng H P, Wang Z G, Lin J, Huang W H, Xu Z Z and Li R X 2004 *Chin. Phys.* **13** 1287
[20] Zuo Z C, Sun J, Liu X, Mi X, Yu Z H, Jiang Q, Fu P M and Wu L A 2007 *Chin. Phys.* **16** 1042
[21] Xue Y, Wang G, Wu J H, Zhang B and Gao J Y 2011 *Chin. Phys. B* **20** 033403
[22] Chen W, Meng Z and Zhou H J 2012 *Chin. Phys. B* **21** 094215
[23] Yang W X, Hou J M and Lee R K 2009 *J. Mod. Opt.* **56** 716
[24] Sun H, Fan S L, Zhang H J and Gong S Q 2013 *Phys. Rev. B* **87** 235310
[25] Phillips M C, Wang H, Rumyantsev I, Kwong N H, Takayama R and Binder R 2003 *Phys. Rev. Lett.* **91** 183602
[26] Wu J H, Gao J Y, Xu J H, Silvestri L, Artoni M, La Rocca G C and Bassani F 2005 *Phys. Rev. Lett.* **95** 057401
[27] Sun H, Niu Y P, Li R, Jin S and Gong S Q 2007 *Opt. Lett.* **32** 2475
[28] Joshi A 2009 *Phys. Rev. B* **79** 115315
[29] Zhu C J and Huang G X 2011 *Opt. Express* **19** 23364
[30] Sun H, Fan S L, Feng X L, Wu C F, Gong S Q, Huang G X and Oh C H 2012 *Opt. Express* **20** 8485
[31] She Y C, Zheng X J, Wang D L and Zhang W X 2013 *Opt. Express* **21** 17393
[32] Hao X Y, Li J H, Liu J B, Song P J and Yang X X 2008 *Phys. Lett. A* **372** 2509
[33] Yang W X and Lee R K 2008 *Opt. Express* **16** 17161